

# Effects of rapid thermal annealing conditions on GaInNAs band gap blueshift and photoluminescence intensity

V. Liverini,<sup>a)</sup> A. Rutz, and U. Keller

ETH Zurich, Physics Department, Institute of Quantum Electronics, Wolfgang-Pauli-Strasse 16, CH-8093 Zürich, Switzerland

S. Schön

ETH Zurich, FIRST Center for Micro- and Nanoscience, Wolfgang-Pauli-Strasse 10, CH-8093 Zürich, Switzerland

(Received 7 December 2005; accepted 3 March 2006; published online 6 June 2006)

We have studied the effects of various conditions of rapid thermal annealing (RTA) on 10 nm GaInNAs/GaAs single quantum wells (SQWs) with fixed indium concentration and increasing nitrogen content to obtain photoluminescence (PL) in the telecom wavelength regime of 1.3 and 1.5  $\mu\text{m}$ . Specifically, we analyzed the results of annealing for a fixed short time but at different temperatures and for longer times at a fixed temperature. In all experiments, InGaAs SQWs with the same In concentration were used as references. For both RTA conditions, the well-known blueshift of the band gap energy and the PL intensity improvement show trends that reveal that these are unrelated effects. At high RTA temperatures the PL efficiency reaches a maximum and then drops independently of N content. On the contrary, the blueshift experiences a rapid increase up to 700 °C (strong blueshift regime) and it saturates above this temperature (weak blueshift regime). Both these blueshift regimes are related to the nitrogen content in the SQWs but in different ways. In the strong blueshift regime, we could obtain activation energy for the blueshift process in the range of 1.25 eV, which increases with N content. Analysis with high-resolution x-ray diffraction (HRXRD) shows that the blueshift experienced in this regime is not due to a stoichiometric change in the QW. In the weak blueshift regime, the blueshift, which is only partly due to In outdiffusion, saturates more slowly the higher the N content. Annealing at the same temperature (600 °C) for a longer time shows that the blueshift saturates earlier than the PL intensity and that samples with higher nitrogen experience a larger blueshift. Only a small In outdiffusion for annealing at high temperatures (>650 °C) and long duration was observed. However, this modest stoichiometric change does not explain the large blueshift experienced by the GaInNAs SQWs. We conclude that the mechanism responsible for the drastic blueshift after annealing is related to the N content in the QW, while the improvement in PL integrated intensity is uniquely related to the annealing conditions.

© 2006 American Institute of Physics. [DOI: [10.1063/1.2200877](https://doi.org/10.1063/1.2200877)]

## I. INTRODUCTION

GaInNAs is a very promising active material for GaAs-based semiconductor lasers in the telecommunication wavelength regime.<sup>1–3</sup> This material still suffers from low photoluminescence (PL) efficiencies even though the incorporation of nitrogen in InGaAs quantum wells (QWs) increases their emission wavelength and reduces the material lattice constant to match it better to GaAs substrates. Very promising was the demonstration that postgrowth (rapid) thermal annealing improves the PL efficiency to values as high as those for nitrogen-free QWs.<sup>4</sup> However, annealing also induces an undesired blueshift of the PL emission wavelength, whose origin is still under investigation. Klar *et al.* propose that this blueshift is caused by nitrogen nearest-neighbors rearrangement during the annealing process.<sup>5</sup> Five configurations of the nitrogen nearest neighbors are possible, starting with one N atom surrounded by four Ga atoms (configuration favored during growth and with the lowest band

gap energy) and continuing with configurations in which the Ga atoms are progressively replaced with In atoms until all of them are substituted (last configuration with the greatest band gap energy). Kondow *et al.* suggest that the unexpected behavior of the band gap in GaInNAs is due to the variation of the strength or length of the GaN bonds. This variation is related to changes in the atomic positions in a unit cell of GaInNAs during the annealing process.<sup>6</sup>

So far no detailed investigation has been published with regards to the blueshift and the improvement in PL efficiency depending on the annealing parameters (i.e., temperature and time duration) and on the initial nitrogen concentration. The results presented here elucidate the effects of the above-mentioned annealing parameters on the PL blueshift and PL integrated intensity improvement and relate them to the nitrogen content.

## II. EXPERIMENTAL PROCEDURE

Our samples consisted of 10 nm Ga<sub>0.65</sub>In<sub>0.35</sub>N<sub>y</sub>As<sub>(1-y)</sub> single quantum wells (SQWs) grown by solid-source molecular beam epitaxy (MBE) on (100) GaAs undoped sub-

<sup>a)</sup>Electronic mail: [liverini@phys.ethz.ch](mailto:liverini@phys.ethz.ch)

strates and capped by a 60 nm GaAs layer. We grew also a N-free SQW at the same growth conditions of the GaInNAs SQWs because it is impossible to determine simultaneously both the N and In concentrations in the SQW by high-resolution X-ray diffraction (HRXRD) due to the fact that In adds compressive strain and N tensile strain, which can compensate each other. For example, a 0.5% increase in In concentration is completely compensated by a 0.2% increase in N concentration. The epitaxy of these SQWs was performed on a GaAs buffer grown at the GaAs deoxidation temperature. During the growth of the buffer layers, the samples temperature was decreased to 450 °C, monitored *in situ* by diffuse reflectance spectroscopy (DRS). This temperature is not optimal for the growth of GaInNAs active material, but was optimized for the growth of the absorber layers used in semiconductor saturable absorber mirrors (SESAMs),<sup>7-9</sup> which were shown to successfully mode-lock 1.3<sup>10</sup> and 1.5  $\mu\text{m}$ <sup>11,12</sup> solid-state lasers. The GaAs cap layer was also grown at this low temperature to prevent *in situ* thermal annealing. The nominal growth rate of the SQWs was 1.2  $\mu\text{m}/\text{h}$  and the As/III beam equivalent pressure (BEP) ratio 22. A VEECO UniBulb RF plasma source was used to incorporate nitrogen in the QWs. We varied the nitrogen incorporation solely by increasing the flow of N from 0.03 to 0.08 sccm (sccm denotes cubic centimeter per minute at STP) and we kept the plasma power constant at 200 W. The nitrogen concentration,  $y$ , obtained by HRXRD, varied from 1.3% to 2.5%. The growth process was observed by reflection high-energy electron diffraction (RHEED). We obtained complete two-dimensional (2D) growth only for the InGaAs SQW and the GaInNAs SQW with lowest N flow. The other SQWs became three dimensional (3D) towards the end on the growth process, however, in all cases the GaAs cap layer recovered the 2D growth mode. The higher the N flow, the earlier the 3D-like behavior started. The room-temperature PL (RT PL) measurements were carried out in a commercial system (Accent RPM 2000). The excitation wavelength and power used were 785 nm and 40 mW, respectively, and the PL was collected via an InGaAs detector. All the samples grown showed as-grown PL increasing from 1350 to 1513 nm in accordance to the nitrogen concentrations measured by HRXRD and reported above. The PL efficiency of the as-grown samples decreased significantly with higher nitrogen incorporation.

For the temperature-dependence studies, six smaller pieces of equivalent size (about  $5 \times 5 \text{ mm}^2$ ) were cleaved after growth from each sample (including the InGaAs SQW sample) to perform rapid thermal annealing (RTA) for 1 min at temperatures ranging from 550 to 800 °C in intervals of 50°. For the time-dependence studies, one more piece was taken from each GaInNAs sample and RTA was performed eight times at 600 °C for times ranging from 1 min up to 40 min per annealing procedure to obtain a total annealing time of 140 min. For comparison, a piece of the InGaAs SQW reference was annealed up to 140 min at 600 °C but in just three annealing procedures. In addition, two pieces (one from the GaInNAs SQW with lowest N and one from the InGaAs SQW) were annealed at 700 °C up to 1 h, mainly to provide the samples with enough energy and time to observe

a significant change in stoichiometry of the SQW. The temperature scale of our commercial RTA apparatus was recently calibrated by monitoring the eutectic point of a 50 nm Al layer deposited on a Si wafer. The annealing processes were performed under N<sub>2</sub> flow and placing a GaAs wafer on top of the samples to provide As overpressure and prevent surface damage due to As evaporation from the GaAs cap layer. The ramp-up rate of the annealing procedure was the same for all samples, 10 K/s up to 50° below the goal temperature and it was lowered to 1/3 of the initial rate for the rest of the ramp-up process to avoid temperature overshoots. The ramp-down rate was much slower. RT PL spectra were always taken before and after annealing to determine the blueshift and change in PL intensity.

Finally, we performed also low-temperature (LT) PL measurements on two selected pieces of the sample with lowest N content, namely, the sample annealed at 750 °C for 1 min and that annealed at 600 °C for 140 min. For this measurement the samples were cooled to liquid He temperature (~4 K) and excited with a 1 mW 483 nm Ar laser. The PL spectrum was collected with a cooled Ge detector and a lock-in amplifier technique was employed for easier detection.

HRXRD rocking curves of the (004) reflex were measured on three samples before and after annealing at 750 °C for 1 min, the InGaAs reference and the two GaInNAs samples with the lowest and highest N incorporation. Moreover, HRXRD scans of the InGaAs sample and the GaInNAs sample with the lowest N content were also taken after annealing at 700 °C for 1 h.

### III. RESULTS AND DISCUSSION

#### A. Effects of different RTA conditions

Figure 1 shows the PL spectra obtained with the two different methods of annealing for the sample with the lowest nitrogen concentration (similar results were obtained for samples with larger N content). Specifically, Fig. 1(a) displays the as-grown and annealed RT PL of a sample annealed at 750 °C for 1 min and Fig. 1(b) that of a sample annealed at 600 °C for 140 min. To make the comparison easier the PL peak intensities have been normalized to the ones of the as-grown samples. Both samples experienced a blueshift of approximately 50 meV and the PL peak intensity improvement is in the same order of magnitude (more than 25 times higher for the annealed samples). At these specific RTA conditions, both methods would seem equivalent to obtain material of the same quality and electronic band gap properties. However, a full analysis of the PL spectral broadening can reveal more about the quality of the material. Several processes, such as slight variations in the quantum well width or composition and structural defects at the interfaces, can broaden the PL spectrum. Therefore, the full width at half maximum (FWHM) of the PL spectrum also gives us an idea about the quality of our material. To get more reliable results for this analysis, we used LT PL with low-intensity pumping. Similarly to the InGaAs material system,<sup>13</sup> we saw a slightly larger FWHM (18 meV compared to 16.4 meV) for the sample annealed at the lower temperature for a longer time.

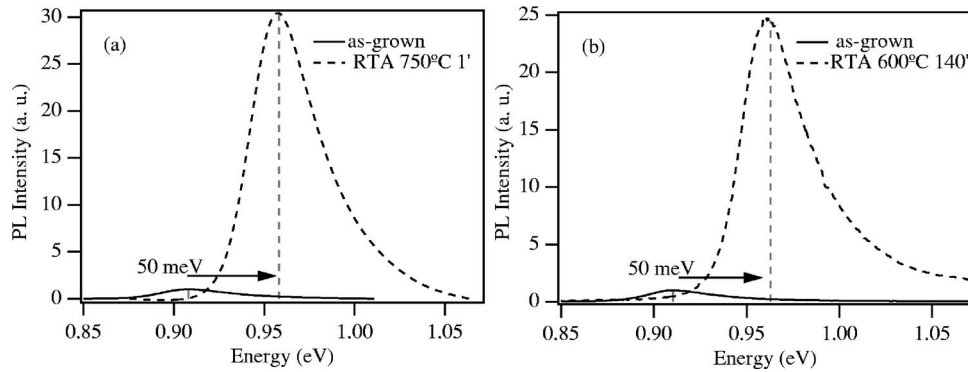


FIG. 1. (a) PL spectra of a 10 nm  $\text{Ga}_{0.65}\text{In}_{0.35}\text{N}_{0.013}\text{As}_{0.987}$  SQW before (solid line) and after (dashed line) RTA for 1 min at 750 °C. (b) PL spectra of a 10 nm  $\text{Ga}_{0.65}\text{In}_{0.35}\text{N}_{0.013}\text{As}_{0.987}$  SQW before (solid line) and after (dashed line) RTA for 140 min at 600 °C.

Therefore, even though both techniques can be used to improve the quality of GaInNAs SQWs, shorter annealing times at higher temperatures are preferable to obtain the best material quality.

## B. Effects of RTA temperature on band gap energy blueshift

### 1. PL analysis

In this section, we report the PL results obtained after performing RTA for a fixed time duration but at different temperatures. Figure 2(a) shows the trend of the energy blueshift,  $\Delta E$ , with annealing temperature for all the GaInNAs samples and the reference InGaAs sample. The first striking feature is that the blueshift of GaInNAs is comparable to that of the InGaAs reference only up to 600 °C, where all samples undergo a blueshift of about 10 meV. The relatively large blueshift in InGaAs at such low temperatures and annealing times is somewhat puzzling. It can be explained by the fact that we are far below the ideal growth temperature

for InGaAs ( $\sim 60^\circ$  below) and that the In atoms cluster at growth temperatures below the ideal one due to lower mobility. This can result in an effective band gap reduction of the as-grown material. At higher annealing temperatures the InGaAs SQW seems unaffected, and only at 800 °C it undergoes a further blueshift of 5 meV. On the other hand, the GaInNAs SQWs continue to blueshift even more with increasing temperature until 700 °C. Up to this point, it appears that all the GaInNAs samples, regardless of composition, behave very similarly, with a final spread in blueshift at 700 °C of only 8 meV. Above this temperature the blueshift starts to level off. From this point on, we will refer to the first blueshift regime, below the RTA temperature of 700 °C, as the “strong blueshift regime” and to the second one, above the RTA temperature of 700 °C, as the “weak blueshift regime.”

In the weak blueshift regime we observe an N-dependent saturation of the blueshift. For easier comparison of the GaInNAs samples with different N concentrations, we made linear fits [gray lines in Fig. 2(a)] of the data points in the

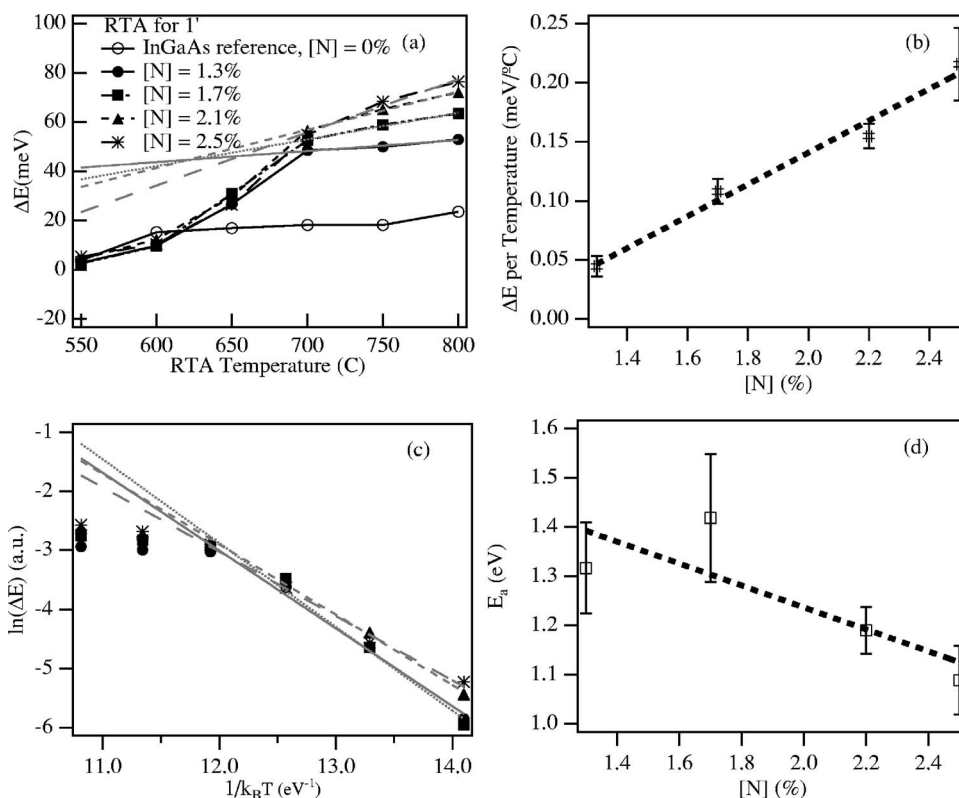


FIG. 2. (a) Energy blueshift,  $\Delta E$ , vs RTA temperature of the GaInNAs SQWs and a reference InGaAs SQW sample with the same In content and same growth conditions. The gray lines are the linear fits of the GaInNAs samples in the weak blueshift regime. (b) Slopes of the linear fits in Fig. 2(a) vs N content (weak blueshift regime). (c) Arrhenius plot of  $\Delta E$  (the InGaAs sample is excluded from this graph). The gray lines are the linear fits in the strong blueshift regime. (d) Activation energy vs N content in the strong blueshift regime.

weak blueshift regime and plotted their slopes versus N content in Fig. 2(b)—the error bars are obtained from the standard deviations of the linear fits. Figure 2(b) clearly shows the trend of samples with higher N content to saturate slower than those with lower N content. This result is in agreement with Klar *et al.*<sup>5</sup> who found that the total blueshift increases with nitrogen concentration.

For the strong blueshift regime, we cannot assume that group III materials outdiffusion is the only process governing the blueshift mechanism (will be explained later). We therefore do not derive the diffusion lengths based on the blueshift itself as commonly done in literature for materials such as InGaAs.<sup>14</sup> In order to establish a quantitative relationship relating the observed blueshift to the N content in the samples, we plotted in Fig. 2(c) the same data as that of Fig. 2(a) in an Arrhenius plot. Then, we fitted the data in the strong blueshift regime as linear fits of the following form:

$$\ln(\Delta E) = \ln(\Delta E_0) - \frac{E_a}{k_B T}, \quad (1)$$

where  $\Delta E_0$  is a constant representing the extrapolated blueshift rate given an infinite high temperature ( $y$  intercept),  $E_a$  the activation energy of the blueshift process,  $T$  the RTA temperature (in Kelvin) and  $k_B$  Boltzmann's constant. The RTA time of 1 min is sufficiently short to justify this approximation. Moreover, calculations of the blueshift rate from the RTA time-dependent studies on selected samples provided the same results.

The slope of the fits [Fig. 2(d)] represents the activation energies for the mechanism that drives the strong blueshift. These activation energies had an average of about 1.25 eV. In Fig. 2(d) we plotted them versus the nitrogen concentration of the as-grown samples. The error bars were again calculated from the estimated standard deviation of the linear fit coefficients. Differently from Fig. 2(c) (slopes of the linear fits in the weak blueshift regime), in Fig. 2(d) the activation energies of this process decrease with increasing N content. This dependence on the nitrogen content implies that less energy is required in material systems with more nitrogen to initiate the drastic blueshift typical of GaInNAs.

## 2. Stoichiometric analysis with HRXRD

We used HRXRD to analyze the composition and shape of the SQWs, before and after annealing in the weak blueshift regime. A possible change of the stoichiometry of the material after annealing, due to In outdiffusion from the SQWs, for example, can contribute to the blueshift observed so far. In Fig. 3 there are two sets of scans, one before and one after annealing at 750 °C for 1 min, for three of the studied samples. The important feature in these scans is the QW peak, i.e., the broad low-intensity peak to the left of the GaAs substrate peak. The distance between the QW peak and GaAs substrate peak corresponds to the perpendicular mismatch, which increases in the pseudomorphically grown layers with increased lattice mismatch of the QW material to the substrate material. When we add In to GaAs to grow InGaAs, we increase the lattice mismatch because the lattice constant of InGaAs increases with In concentration. Adding

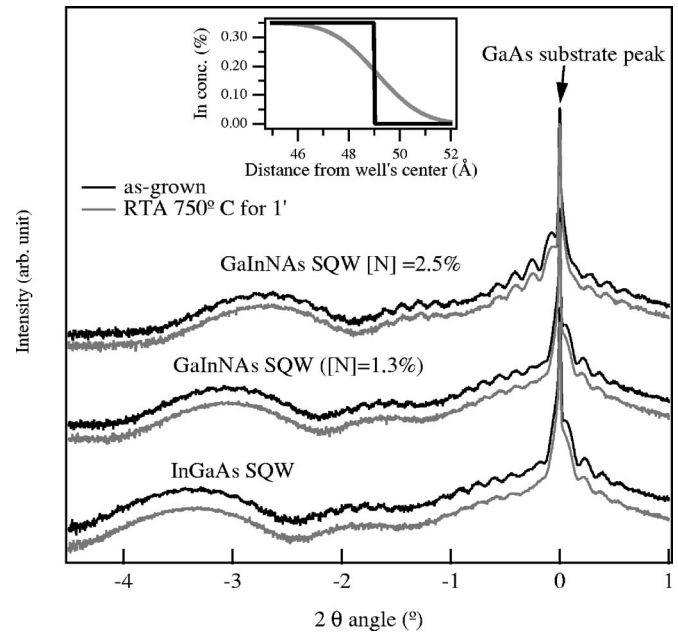


FIG. 3. HRXRD of the samples with various N content before (black lines) and after (gray lines) annealing at 750 °C for 1 min. Inset: In profile in the as-grown SQW (black line) and error function profile (gray line) of the outdiffused quantum well with 2 Å diffusion length.

N to InGaAs, instead, reduces the lattice mismatch. In fact, we see in the as-grown XRD scans (black lines) that the most strained material (highest perpendicular mismatch) is the InGaAs SQW. The more N we add, the closer the QW peak moves towards the GaAs substrate peak. Therefore, the position of the QW peak tells us the stoichiometry of the QW. The width of the QW peak corresponds to the thickness of the QW in reciprocal space, therefore the smaller the width, the thicker the QW. The annealed samples (gray lines) do not appear to show neither a change in the position of the QW peak nor in its width. This implies that no apparent change in the stoichiometry of the materials is present neither for InGaAs nor for the GaInNAs samples—at least for the accuracy of an HRXRD measurement. Based on their experimental outcomes on the kinetics of compositional disorder in the InGaAs/GaAs material system, Tsang *et al.* proposed an equation for the intrinsic diffusivity  $D_{\text{In-Ga}}$  with respect to temperature.<sup>15</sup> Following their results, we found the expected diffusion length of a SQW exposed to RTA at 750 °C for 1 min to be approximately 2 Å. The inset in Fig. 3 shows the difference between the as-grown profile (black line) and the error function profile (gray line) of a SQW from which In outdiffused by 2 Å. The annealed samples scans could be fitted equally well with the as-grown profile as with the error function profile, meaning that the 2 Å diffusion length is too small to be noticed in the HRXRD. The only clear difference between the annealed and as-grown samples is that the small Pendellösung fringes in Fig. 3 nearly disappear around the QW peak. However, they are still visible around the GaAs peak. These fringes are related to the thickness of the GaAs cap layer. Because they have the same periodicity before and after RTA, their lower visibility is not due to the loss of the GaAs cap but to surface roughness generated during annealing. This is further confirmed by phase-contrast microscopy, which makes the roughness easily visible.

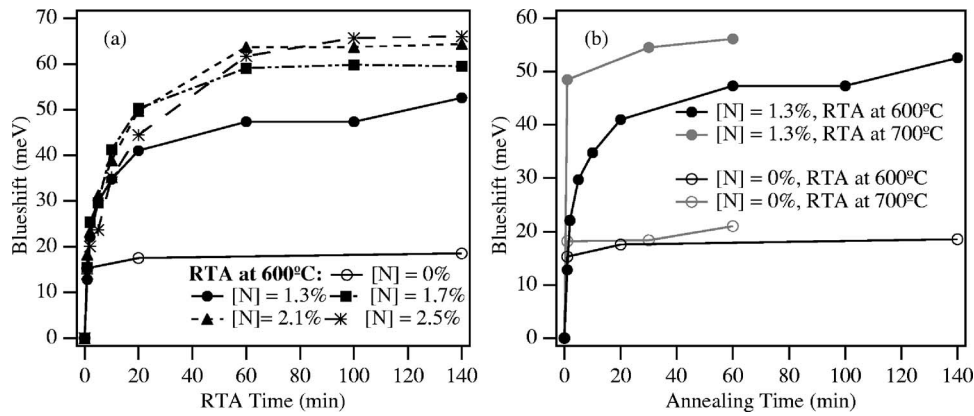


FIG. 4. Blueshift vs RTA time of the GaInNAs SQWs and a reference InGaAs SQW sample with the same In content and same growth conditions. (a) Data for RTA at 600 °C. (b) Data for the InGaAs sample (open circles) and the GaInNAs sample with lowest N content (solid circles) at the RTA temperature of 600 °C (black lines) and 700 °C (gray lines).

### 3. Conclusion of PL and HRXRD analyses

To summarize the results on the effects of RTA temperature on band gap energy blueshift, we can reach the following conclusions. We cannot attribute the strong blueshift experienced by the samples annealed in the strong blueshift regime (i.e., at low RTA temperatures) to In outdiffusion because we do not see more than a 2 Å In outdiffusion length due to the RTA process for the weak blueshift regime (i.e., at high RTA temperatures). This is also evidenced by the great difference between the blueshift experienced by the GaInNAs SQWs and the InGaAs SQW [Fig. 2(a)]. The blueshift in this regime must be due to another process that does not involve a stoichiometric change of the QW. On the other hand, from our HRXRD analysis of the samples in the weak blueshift regime (Sec. III B 2), we cannot exclude that also a small initial In outdiffusion is occurring.

## C. Effects of RTA time on band gap energy blueshift

### 1. PL analysis

In this section we report the results obtained for RTA experiments in which the temperature was kept constant and the annealing time increased to more than 1 min. Figure 4(a) shows the trend of the blueshift with respect to annealing time for samples annealed at 600 °C. At the beginning all the GaInNAs samples experience a strong blueshift and no real trend can be distinguished between the samples with different nitrogen content. However, after 1 h annealing, the blueshift saturates and again we see that samples with more N content experience a higher blueshift than the samples with lower N content. In contrast, the reference InGaAs sample, which experiences a blueshift comparable to that of the GaInNAs samples only for the first 1 min, saturates much earlier to a significantly lower blueshift.

We performed another annealing experiment on the InGaAs SQW and the GaInNAs SQW with lowest N content at 700 °C. For comparison purposes, the results are shown in Fig. 4(b) (gray) together with the results at 600 °C for the same samples already shown in Fig. 4(a) (black). The InGaAs SQWs blueshift was quite similar independently of annealing temperature, i.e., most of the blueshift occurred within the first minute and longer annealing at the same temperature did not affect the blueshift considerably more. However, the situation is quite different for the GaInNAs SQW. In this case, already after 1 min annealing at 700 °C results

in a blueshift three times as large as at 600 °C. Then, the extra blueshift from 1 min to 1 h at 700 °C is only of ~8 meV compared to the much more gradually increasing blueshift at 600 °C, where the extra blueshift is ~35 meV. In Fig. 4(b) we can also clearly see that both annealing temperatures tend to saturate to a similar level (comparison between gray and black solid dots). We therefore conclude that the blueshift saturation condition can be obtained at any annealing temperature as long as enough time is provided.

### 2. Stoichiometric analysis with HRXRD

An HRXRD analysis of the samples after annealing [Fig. 5(a)] shows for both the InGaAs sample and the GaInNAs sample a shift of the QW peak towards the GaAs substrate peak and a narrowing of its width. A reduced contrast of the Pendellösung fringes on the QW peak (as observed in Fig. 3) is in this case also accompanied by a broadening of the GaAs substrate peak. This occurs for both the InGaAs and the GaInNAs SQWs. We were able to fit the x-ray scan of the InGaAs sample with both a square well profile and an error function profile [Fig. 5(b)]. The square quantum well fit (gray solid line) resulted in a 4 Å larger SQW with about 0.8% less indium. The error function profile fit (dashed gray line) resulted in an In outdiffusion length of about 8 Å. This diffusion length is in agreement with the value predicted by Tsang *et al.*<sup>15</sup> for these annealing conditions. The last few nanometers of the profiles for these fit functions are shown in the inset in Fig. 5(b). Considering that neither fit is perfect, we cannot conclusively prefer one to the other. However, both fits clearly attribute the QW peak shift to In outdiffusion. We included the results obtained with the simple square well mode because it is still under discussion if it is valid to assume a Fickian diffusion with a constant diffusion coefficient and to use the error function profile approach for In outdiffusion. In fact, other researchers have also found that a simple square fit profile can also be employed successfully for this analysis.<sup>16</sup> For completeness we must add that neither fit can satisfactorily reproduce the GaAs peak's broadening, which is probably due to the damage of the GaAs cap layer observed after the long-time annealing at 700 °C of all our samples. Such damage does not occur in samples annealed at 600 °C regardless of annealing duration, and HRXRD scans of these samples do not exhibit a broadened substrate peak.

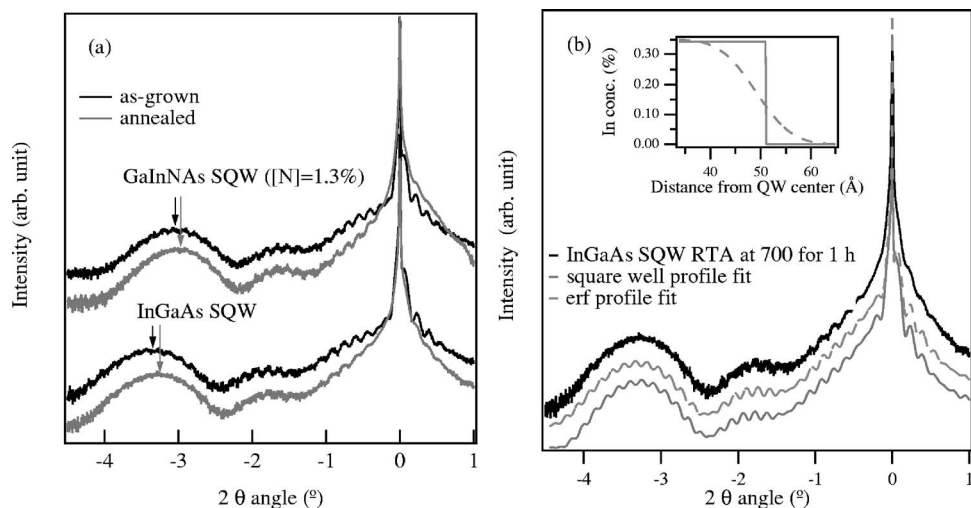


FIG. 5. (a) HRXRD of GaInNAs SQW and reference InGaAs SQW before (black lines) and after (gray lines) annealing at 700 °C for 1 h. (b) HRXRD of reference InGaAs SQW after annealing at 700 °C for 1 h (black line), square well fit (solid gray line) with 0.8% less In and 4 Å larger quantum well than the as-grown sample and error function profile fit (dashed gray line) with an assumed diffusion length of 8 Å. Inset: In profile of the square fit (solid gray line) and of the error function profile fit (dashed gray line).

In the case of the GaInNAs SQW, after annealing we see a shift of the QW peak, which is of the same magnitude and in the same direction as that observed for the InGaAs SQW [Fig. 5(a)]. Also in this case we can fit the XRD curve by assuming a 4 Å increase in the thickness and a decrease of 0.8% in the In content of the well. There was no need to assume loss of N, which could account for the larger blueshift observed for GaInNAs compared to InGaAs in Fig. 4(b).

#### D. Effects of RTA time and temperature on PL intensity

Annealing GaInNAs not only produces a drastic blueshift but also greatly improves the material quality with a reduction of nonradiative defects. This is revealed by the significant increase in the PL intensity after RTA (Fig. 1). It is more appropriate to analyze the integrated intensity of the PL spectrum over energy than just its peak intensity because after the annealing process the shape of the PL spectrum is usually altered, for example by changes in the spectral width. We further define the PL integrated intensity improvement,  $\eta$ , as the ratio between the PL integrated intensity of the annealed sample normalized by that of the as-grown sample. The results for the analyzed SQWs are shown in Fig. 6. In Fig. 6(a),  $\eta$  for samples annealed at the set of temperatures defined in the experimental procedure can be seen. Up until 600 °C annealing, all samples behave very similarly (i.e., no real trend can be seen with N content), and show an  $\eta$  below

five times the original intensity. Also Fig. 2(a) shows that the blueshift for all samples is relatively small and similar for temperatures below 600 °C. In contrast to the InGaAs sample, the GaInNAs samples exhibit an optimal annealing temperature of 700–750 °C with a clear maximum in  $\eta$ . Annealing at even higher temperatures saturates the improvement quite quickly, which is probably due to surface damage of the GaAs cap. This is a limitation of the *ex situ* annealing method, which can be overcome by *in situ* annealing.

As mentioned earlier, GaInNAs samples with higher nitrogen content have lower as-grown PL integrated intensities, which means that the samples with more nitrogen have more nonradiative centers. At the end of the annealing process samples with more nitrogen still have lower PL integrated intensities compared to the others. In Fig. 6(a) we can see that the GaInNAs samples all experienced an  $\eta$ , which falls in the same range within the error bars. Therefore, no clear trend with N concentration can be observed. The same conclusion can be drawn from Fig. 6(b), where  $\eta$  versus annealing time for samples annealed at 600 °C is shown. As long as the number of nonradiative defects incorporated during growth is very large, the improvement provided through annealing will be limited. This measurement confirms the difficult situation for the samples with high N content even after postgrowth annealing treatment. Thus, this gives some stronger indications that solutions for how to obtain better material properties must be looked for in the actual growth con-

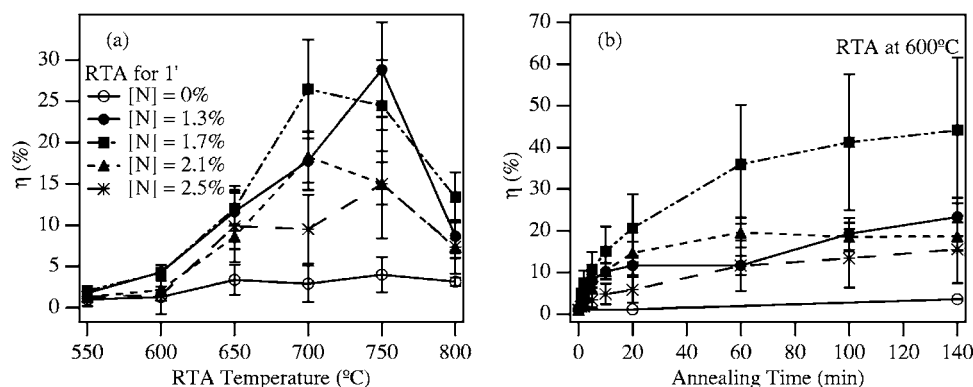


FIG. 6. PL integrated intensity improvement of the GaInNAs SQWs and a reference InGaAs SQW sample with the same In content and same growth conditions (a) vs RTA temperature for 1 min annealing, (b) vs RTA time at the annealing temperature of 600°.

ditions of this complex quaternary material. In Fig. 6(b) it can also be noted that the PL integrated intensity improvement is not quite saturated yet, while the blueshift is [Fig. 4(a)]. For longer times more improvement it is still possible but at the expenses of the PL FWHM, which starts increasing after one hour annealing even at low temperatures.

#### IV. CONCLUSIONS

We report the results of systematic studies of rapid thermal annealing of GaInNAs SQWs with different N content with PL emission wavelength from 1.3 to 1.5  $\mu\text{m}$ . We show that short annealing for 1 min at different temperatures results in a blueshift trend that can be divided in two regimes: a strong blueshift regime, up to 700 °C, where the SQWs blueshift decreases quite drastically with annealing temperature, and a weak blueshift regime, above 700 °C, where the blueshift increases more slowly with RTA temperature, i.e., the blueshift saturates. In the latter regime, the samples with larger N content saturate more slowly than those with lower N content. For the strong blueshift regime, we used an Arrhenius-type model to calculate the activation energy of the blueshift mechanism and found that all N-containing samples had activation energies from 1.09 to 1.32 eV, which increased with decreasing N content. These results imply that more nitrogen allows for easier initiation of the blueshift process and slower blueshift saturation. HRXRD analysis shows that this drastic blueshift cannot be justified by In outdiffusing from the quantum well during short time annealing in the strong blueshift regime. Only in the weak blueshift regime, In outdiffusion is also responsible for the blueshift. In contrast to the blueshift, the PL integrated intensity improvement of the samples did not depend on the nitrogen content. In general, samples with more nitrogen have lower as-grown PL integrated intensity. Annealing partially heals their as-grown nonradiative defects but they remain with PL intensities lower than samples with less N.

Annealing at a fixed temperature for longer times results in the same total saturated blueshift encountered when annealing at different temperatures. The annealing temperature determines only how fast the blueshift saturates. For long-term annealing at 700 °C we do observe as much In outdiffusion as in a reference InGaAs SQW, which still cannot be accounted for the only cause for the larger blueshift observed

in GaInNAs. In contrast to the blueshift, the PL integrated intensity improvement saturates more slowly with annealing at relatively low temperatures for longer times. However, this improvement comes at the expense of an increased PL FWHM for longer annealing times. Therefore, in practice, short-time annealing at high temperatures is preferable to long-time annealing at low temperatures. Finally, we believe that more substantial improvement in the quality of GaInNAs will depend not only on optimized postgrowth annealing, but also on growth conditions devised to be very sensitive to postgrowth annealing.

#### ACKNOWLEDGMENTS

We would like to thank Dr. Hans Sigg from the PSI for his support with the low-temperature PL measurements. We are also grateful to Dr. Markus Haiml, Rachel Grange, and Simon C. Zeller for helpful discussions on this topic. In addition, we would like to acknowledge the financial support of the NCCR in quantum photonics.

- <sup>1</sup>M. Kondow, K. Uomi, A. Niwa, T. Kitatani, S. Watahiki, and Y. Yazawa, *Jpn. J. Appl. Phys., Part 1* **35**, 1273 (1996).
- <sup>2</sup>M. Fischer, D. Gollub, M. Reinhardt, M. Kamp, and A. Forchel, *J. Cryst. Growth* **251**, 353 (2003).
- <sup>3</sup>H. Riechert, A. Ramakrishnan, and G. Steinle, *Semicond. Sci. Technol.* **17**, 892 (2002).
- <sup>4</sup>H. P. Xin, K. L. Kavanagh, M. Kondow, and C.-W. Tu, *J. Cryst. Growth* **201–202**, 419 (1999).
- <sup>5</sup>P. J. Klar *et al.*, *Phys. Rev. B* **64**, 121203 (2001).
- <sup>6</sup>M. Kondow, T. Kitatani, and S. Shirakata, *J. Phys.: Condens. Matter* **16**, S3229-44 (2004).
- <sup>7</sup>U. Keller, D. A. B. Miller, G. D. Boyd, T. H. Chiu, J. F. Ferguson, and M. T. Asom, *Opt. Lett.* **17**, 505 (1992).
- <sup>8</sup>U. Keller *et al.*, *IEEE J. Sel. Top. Quantum Electron.* **2**, 435 (1996).
- <sup>9</sup>U. Keller, *Nature (London)* **424**, 831 (2003).
- <sup>10</sup>V. Liverini, S. Schön, R. Grange, M. Haiml, S. C. Zeller, and U. Keller, *Appl. Phys. Lett.* **84**, 4002 (2004).
- <sup>11</sup>A. Rutz, R. Grange, V. Liverini, M. Haiml, S. Schön, and U. Keller, *Electron. Lett.* **41**, 321 (2005).
- <sup>12</sup>S. Schön, A. Rutz, V. Liverini, R. Grange, M. Haiml, S. C. Zeller, and U. Keller, *J. Cryst. Growth* **278**, 239 (2004).
- <sup>13</sup>G. P. Kothiyal, P. Bhattacharya, *J. Appl. Phys.* **63**, 2760 (1988).
- <sup>14</sup>W. P. D. Gillin, D. J. Dunstan, K. P. Homewood, L. K. Howard, and B. J. Sealy, *J. Appl. Phys.* **73**, 3782 (1993).
- <sup>15</sup>J. S. L. Tsang, C.P. Lee, S. H. Lee, K. L. Tsai, C. M. Tsai, and J. C. Fan, *J. Appl. Phys.* **79**, 664 (1996).
- <sup>16</sup>F. Bollet, W. P. Gillin, M. Hopkinson, and R. Gwilliam, *J. Appl. Phys.* **97**, 013536 (2005).